PHYSICAL REVIEW B **80**, 081310(R) (2009)

Direct observation of the structure of band-edge biexcitons in colloidal semiconductor CdSe quantum dots

Samuel L. Sewall,[1] Alberto Franceschetti,[2,*] Ryan R. Cooney,[1] Alex Zunger,[2,*] and Patanjali Kambhampati[1,*]
[1]*Department of Chemistry, McGill University, Montreal, Quebec, Canada H3A 2K6*
[2]*National Renewable Energy Laboratory, Golden, Colorado 80401, USA*
(Received 5 August 2009; published 25 August 2009)

We report on the electronic structure of the band-edge biexciton in colloidal CdSe quantum dots using femtosecond spectroscopy and atomistic many-body pseudopotential calculations. Time-resolved spectroscopy shows that optical transitions between excitonic and biexcitonic states are distinct for absorptive and emissive transitions, leading to a larger Stokes shift for the biexciton than for the single exciton. The calculations explain the experimental results by showing that there is a previously unobserved electronic substructure to the band-edge biexciton which yields two distinct families of transitions.

DOI: 10.1103/PhysRevB.80.081310 PACS number(s): 78.67.Hc, 73.21.La, 73.22.−f, 82.53.Mj

Physical confinement of electrons and holes in semiconductor quantum dots yields the well-known quantization of excitonic states.[1] The energy spectrum of the *single exciton* (X) is characterized by a coarse as well as a fine structure.[1–6] While the coarse structure arises primarily from quantum confinement and spin-orbit interactions and is manifested in higher absorption bands above the band edge, the fine structure originates from electron-hole exchange interactions and lattice asymmetries, and results in an energy shift between absorbing transitions and emitting transitions.

In addition to single excitons, quantum dots are known to support quantum-confined excitonic *complexes*.[1] The simplest excitonic complex is the neutral biexciton (XX), consisting of two electrons and two holes. Current efforts to investigate excitonic complexes[1,7–15] are motivated by a desire to understand the fundamental physics of carrier interactions in nanostructures, as well as by potential applications based on optical gain[1,7,16,17] and multiple exciton generation[18–20] phenomena.

The structure of excitonic complexes is relatively well explored in self-assembled epitaxial dots and dots grown on prepatterned substrates.[11,15,18–22] However, there is still little understanding of the electronic structure of biexciton complexes in the complementary case of colloidal quantum dots—systems characterized by significantly different electronic structure, selection rules, relaxation time scales and pathways, and interaction energies. The electronic structure of the biexciton plays a central role in the physics underpinning optical gain[7,16] and in the recently observed multiple exciton generation process.[23–25] In the development of gain via optical pumping, it is the interplay between stimulated emission from the biexciton and excited state absorption into the biexciton which controls the balance between gain and loss.[7,16] This balance should be entirely determined by the substructure to the biexciton—a quantity yet to be investigated in colloidal quantum dots. In the case of multiple exciton generation, it is the density of final biexciton states which determines the efficiency of this process.[23–25] Yet there is no experimental observation of the spectrum of the biexciton.

Here, we show that the band-edge biexciton in colloidal quantum dots does indeed possess a unique previously unobserved electronic structure. We demonstrate the existence of such structure using femtosecond spectroscopy and assign the physical origin of the observed optical transitions using atomistic pseudopotential calculations. We find that the substructure of the band-edge biexciton is fundamentally distinct in origin from the substructure of the single exciton. As a result, the transitions between excitonic and biexcitonic states are distinct for absorptive and emissive spectroscopies, yielding an observation of a biexciton Stokes shift.

In this work, we will focus on the substructure of the band-edge biexciton ($1S_h+1S_e$) in CdSe colloidal nanocrystals. Figure 1 shows schematically the single-particle energy levels (part a), the multiparticle X and XX energy levels and related optical transitions (part b), as well as the main measurable quantities (part c). We will use this figure throughout the Rapid Communication to define all of the quantities discussed both experimentally and theoretically. The S-like hole states at the top of the valence band [h_1 and h_2 in Fig. 1(a)] originate from the bulk Γ_{9v} and Γ_{7v} band states and are split by the crystal field due to the hexagonal wurtzite lattice structure and by deviations from the spherical shape. They are followed by the P-like hole states h_3 and h_4. The S-like electron state at the bottom of the conduction band [e_1 in Fig. 1(a)] originates from the bulk Γ_{7c} band state and is followed by three nearly degenerate P-like electron states (e_2-e_4).

The way in which the single-exciton fine structure evolves from these single-particle orbitals has been explained previously[1–5] and is shown schematically in Fig. 1(b). The X fine structure consist of two manifolds of four states each, originating from the (h_1,e_1) and (h_2,e_1) exciton configurations, respectively. The lowest exciton level of each manifold is dark, leaving three dipole-allowed optical transitions [denoted A_1, A_2, and A_3in Fig. 1(c)].

This energy-level structure manifests itself in experiment via Stokes shifts. The resonant X Stokes shift is caused by absorption into the bright state (A_1 transition) and emission from the dark state below it. The global X Stokes shift $\delta_X = E_X^{abs} - E_X^{emi}$ [where E_X^{abs} denotes the energy of the lowest X absorption peak and E_X^{emi} the energy of the X emission peak, see Fig. 1(c)] originates from contributions of higher-energy transitions (A_2 and A_3) to the absorption peak and from phonon-progression contributions to the absorption and emission peaks.[1–3]

The lowest-energy manifold of biexciton states originates

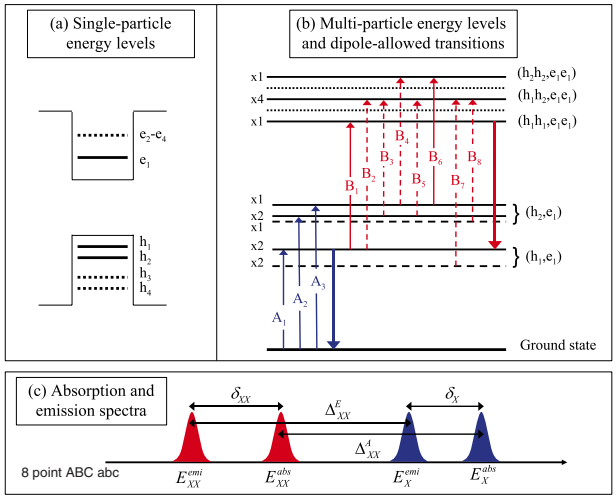

FIG. 1. (Color online) Schematic depiction of all calculated and measured spectroscopic quantities for a wurtzite CdSe nanocrystal: (a) single-particle band-edge energy levels. (b) Exciton and biexciton states originating from the *S*-like hole states h_1 and h_2 and the electron state e_1. The degeneracy of the exciton states is shown on the left-hand side, while the primary single-particle configuration from which the exciton originates is shown on the right-hand side. In the case of *X*, solid horizontal lines indicate spin-allowed states, dashed lines indicate spin-forbidden states. In the case of *XX*, dotted horizontal lines indicate states originating from the *P*-like hole states h_3 and h_4, which do not contribute to the low-energy optically allowed transitions. Vertical arrows denote dipole-allowed absorption transitions and room-temperature emission transitions. The $X \rightarrow XX$ transitions can be further classified (see text) as strong (solid-line arrows) or weak (dashed-line arrows). (c) Schematic plot of the *X* and *XX* absorption peaks (E_X^{abs} and E_{XX}^{abs}) and emission peaks (E_X^{emi} and E_{XX}^{emi}).

from the *S*-like (h_1h_1,e_1e_1), (h_1h_2,e_1e_1), and (h_2h_2,e_1e_1) configurations of two hole and two electron orbitals [Fig. 1(b)]. The *XX* ground state (h_1h_1,e_1e_1) has a closed-shell *S*-like configuration so a resonant Stokes shift of the type observed for the single exciton—due to exchange-induced bright/dark splitting—cannot exist for the biexciton. However, as in the case of *X*, a *global XX* Stokes shift $\delta_{XX}=E_{XX}^{abs}-E_{XX}^{emi}$ [where E_{XX}^{abs} denotes the energy of the lowest *XX* absorption peak and E_{XX}^{emi} the energy of the *XX* emission peak, see Fig. 1(c)] may arise from the contribution of higher-energy transitions [e.g., B_4 and B_6 in Fig. 1(b)] to the absorption peak. Furthermore, the existence of split hole states h_1 and h_2 [Fig. 1(a)] creates a distinction between "direct" transitions such as $X(h_1,e_1)\rightarrow XX(h_1h_1,e_1e_1)$ and "indirect" transitions such as $X(h_1,e_1)\rightarrow XX(h_1h_2,e_1e_1)$. One may expect that direct transitions will be stronger and higher in energy than indirect transitions, hence opening the possibility of a peculiar contribution to the global *XX* Stokes shift.

It is also useful to define the *intrinsic* biexciton binding energy $\Delta_{XX}=2E_X^0-E_{XX}^0$, i.e., the difference between twice the *X* ground-state energy E_X^0 and the *XX* ground-state energy E_{XX}^0. This quantity can be calculated[14] but requires high-energy resolution (at the expense of time resolution) to measure. Instead, experiments typically detect the *apparent* biexciton binding energy, i.e., the difference between the *XX* and *X* peaks, measured either in absorption ($\Delta_{XX}^A=E_X^{abs}-E_{XX}^{abs}$) or in emission ($\Delta_{XX}^E=E_X^{emi}-E_{XX}^{emi}$), as shown schematically in Fig. 1(c). These apparent binding energies are naturally different from the intrinsic binding energies.

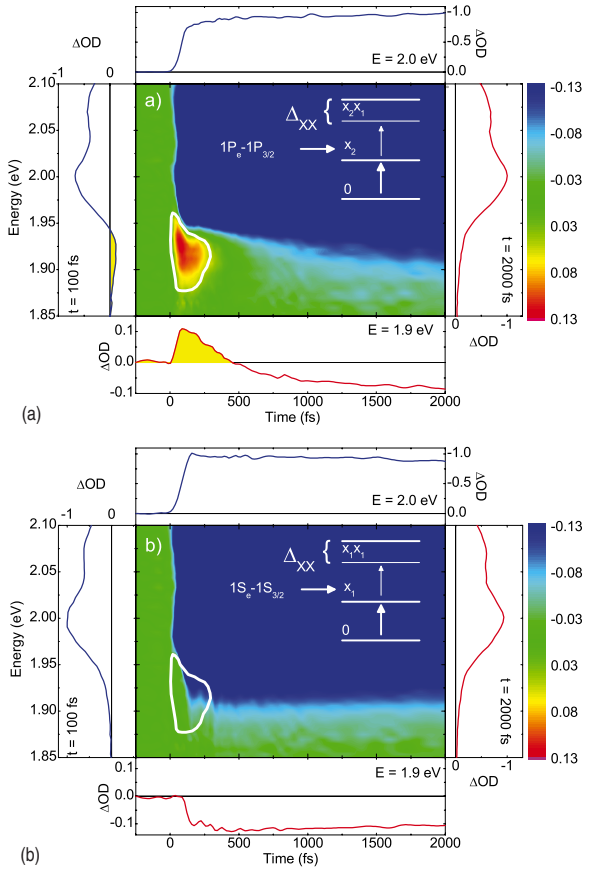

FIG. 2. (Color online) Signature of biexcitons in absorptive experiments. Panel (a) shows the transient absorption (TA) data of CdSe quantum dots upon pumping into the 1P exciton, while panel (b) shows TA data upon pumping into the 1*S* band-edge exciton: $E=2.00$ eV and $R=2.8$ nm. The contour plots have a truncated *z* axis in order to highlight the biexcitonic signal (circled). Projections along the energy and time axes are provided for two values of probed energy and time delay.

Transient absorption (TA) experiments can detect bound biexcitons by the presence of induced absorptions in the transient spectrum.[1,12,13,26] The pump pulse produces a single exciton, and the probe pulse follows the system into the biexciton. The biexciton interactions shift the level structure yielding new absorptive features in the TA spectrum. The state-resolved spectroscopic measurements were made in the pump/probe configuration with 10 fs precision, the details of which were previously described.[12,13,16,26] The sample consisted of CdSe quantum dots dispersed in toluene and flowed at 300 K.

Figure 2 shows TA experiments in strongly confined CdSe quantum dots upon pumping into two different initial excitonic states ($R=2.8$ nm, band-edge exciton at 2.00 eV). Upon excitation into the 1*P* exciton [corresponding to a hole in the h_3-h_4 states and an electron in the e_2-e_4 states, see Fig. 1(a)] one observes the induced absorption expected[1,12,13] in the TA spectrum [Fig. 2(a)]. The induced absorption is circled and the *z*-axis (ΔOD) is truncated in order to more clearly focus in on the induced absorption which is subreso-

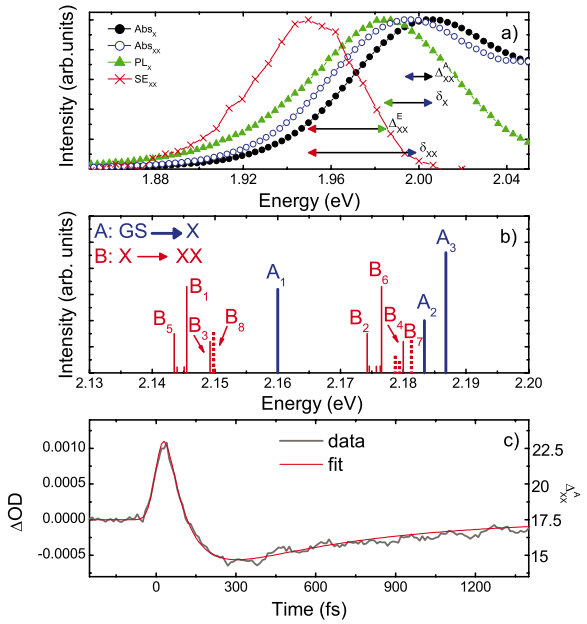

FIG. 3. (Color online) Biexcitonic signatures in absorptive and emissive experiments. (a) Comparison of absorptive and emissive experiments at the single exciton and biexciton level. The biexciton binding energies are not the same in absorptive (Δ_{XX}^{A}) and emissive (Δ_{XX}^{E}) experiments. The Stokes shift structure for the biexciton (δ_{XX}) is not the same as for the single exciton (δ_X). (b) Calculated energies and intensities of the GS$\rightarrow X$ (A_1-A_3) and $X\rightarrow XX$ (B_1-B_8) low-energy optical transitions for a 1.9 nm CdSe nanocrystal. In the case of $X\rightarrow XX$ absorption, solid lines indicate transitions originating from dipole-allowed (bright) X states, while dashed lines indicate transitions from dipole-forbidden (dark) X states. (c) Time evolution in absorptive experiments, revealing the shifting apparent binding energy.

nant to the band-edge exciton. The contour plot has projections along the time and energy axes in order to show slices of the transient spectra and dynamics without truncation of the ΔOD axis. In stark contrast, pumping into the $1S$ band-edge exciton (hole in the h_1-h_2 states and electron in the e_1 state) shows a clear *absence* of the expected induced absorption [Fig. 2(b)] due to the balance between state filling and level shifting in the optical signal.[13] The main point is that pump and probe pulses can be chosen to probe signals which correspond to *specific* biexcitonic states, a point we have discussed previously.[12,13,16]

The XX apparent binding energy in colloidal CdSe quantum dots was previously measured using both absorptive[1,12,13] and emissive[1,8–10] experiments, yielding the quantities Δ_{XX}^{A} and Δ_{XX}^{E}, respectively. Under conditions of band-edge pumping, Δ_{XX}^{A} is small but measurable. The excited states are more strongly bound, a point which will be discussed elsewhere. The XX apparent binding energy Δ_{XX}^{A} $\sim$8.5 meV is much smaller than published values (30–40 meV) based upon transient emission experiments.

In order to assess whether these differences are artificial or fundamental, we performed emissive experiments with the same femtosecond time resolution. Figure 3(a) shows the linear as well as nonlinear time-resolved spectra for both absorptive and emissive experiment upon pumping into the band-edge exciton. Since the pump is resonant with the band-edge exciton, there can only be two excitons populated by the pump pulse.[1,16,17] The stimulated emission (SE) spectrum (at 1 ps) corresponds to the negative portion of the nonlinear absorption spectrum ($\mathrm{OD_{NL}}=\Delta\mathrm{OD}+\mathrm{OD_0}$).[7,16,17] Δ_{XX}^{emi} is the energy difference between the maximum of the SE spectrum and the maximum of the photoluminescence (PL) spectrum represents the same ground-state biexciton obtained in the emissive experiments.[1,8–10] Our value of $\Delta_{XX}^{E}=36$ meV is consistent with prior emissive measurements of biexcitons.

The significant energy difference between the absorptive and emissive apparent binding energies Δ_{XX}^{A} and Δ_{XX}^{E} implies that the magnitude of the global XX Stokes shift (δ_{XX}) is different from that of the global X Stokes shift (δ_X). The XX Stokes shift is nontrivial in that it does not arise from the same electronic substructure that produces the single-exciton Stokes shift. The experimental values of Δ_{XX}^{A}, Δ_{XX}^{E}, δ_X, and δ_{XX} can be extracted from the data in Fig. 3(a).[26] For three quantum-dot sizes, $R=(1.5,2.1,2.8)$ nm, we obtain $\Delta_{XX}^{A}=(18,12,9)$ meV, $\Delta_{XX}^{E}=(50,44,37)$ meV, $\delta_X=(40,25,16)$ meV, and $\delta_{XX}=(73,57,45)$ meV. Our *emissive* experiments reproduce the results of prior emissive experiments, but our *absorptive* experiments yield markedly different apparent binding energies. These experiments reveal a biexciton Stokes shift which is not the same as the single exciton Stokes shift.

Calculations of the X and XX energy levels and transitions were performed using the semiempirical pseudopotential approach described in Ref. 5. We considered nearly spherical CdSe nanocrystals of radius $R=1.9$ and 2.3 nm, whose surfaces were passivated using ligand potentials.[5] Figure 3(b) shows the calculated individual GS$\rightarrow X$ and $X\rightarrow XX$ transition energies and their oscillator strengths (GS denotes the electronic ground state) for a $R=1.9$ nm CdSe nanocrystal. As shown in Fig. 1(b), there are three GS$\rightarrow X$ transitions and eight main $X\rightarrow XX$ transitions, all of which are labeled in Fig. 3(b). These individual X and XX absorption and emission lines are currently not observed experimentally because of limited energy resolution (line broadening of spectra and the laser bandwidth required to maintain fs time resolution). Thus, to mimic the experimental situation, we calculated the absorption and emission spectra using a Gaussian line broadening of 100 meV, similar to the inhomogeneous broadening of an ensemble of the highest quality CdSe quantum dots at 300 K. We further note that the broadenings do not prevent insight into the electronic structure since the level shiftings are very large (10–70 meV).

The calculations were performed at $T\sim 0$ and $T=300$ K. The temperature affects the population of the X and XX sublevels, but the energies of the single-particle levels are assumed to be temperature independent (except for the change in the band gap with temperature). In the case of the $X\rightarrow XX$ absorption spectrum, the initial X states were populated in two different ways: (i) according to the Boltzmann distribution, starting from the lowest-energy X state and (ii) according to their normalized oscillator strengths. These two choices correspond to long and short pump/probe delay times, respectively. From the calculated absorption and emis-

sion spectra, we extracted the global Stokes shifts δ_X and δ_{XX}, and the apparent binding energies Δ_{XX}^A and Δ_{XX}^E, which are summarized in Table I in the supplementary information.[26]

The main result is that both δ_X and δ_{XX} have a significant electronic (i.e., non-phonon-induced) component.[26] At $T=300$ K, the calculated δ_X is 8–9 meV for the two CdSe nanocrystals considered here, whereas δ_{XX} is 14–16 meV. As T decreases, δ_X increases to 22 meV (18 meV) for $R=1.9$ nm (2.3 nm). This is due to the change in the position of the emission peak as higher-energy X states become depopulated. At low temperature, δ_{XX} depends very sensitively on the delay time Δt. For short pump/probe delay times δ_{XX} is 12–14 meV, whereas for long pump/probe delay times $\delta_{XX}=33-35$ meV. This behavior can be rationalized by observing that at $T\sim 0$ and $\Delta t \gg 1$ ps the system is in the X "dark" state. Transition from this state to the XX ground state (h_1h_1,e_1e_1) are spin forbidden. Only transitions to the XX excited state (h_1h_2,e_1e_1) are dipole allowed [B_7 in Figs. 1(b) and 3(b)]. This selection rule shifts the center of the absorption peak to higher energy and therefore increases δ_{XX}. Thus, the calculations predict that the global XX Stokes shift and the apparent XX binding energy (but not the actual binding energy) should be *time-dependent* quantities. The time dependence arises as the optically coupled bright states relax to their Boltzmann distributions. Experiments on the smallest dot confirm these predictions [see Fig. 3(c)]. These dynamics are due to relaxation from the optically coupled exciton states to the relaxed thermally populated exciton states. The relaxation takes place on the 80 fs time scale, consistent with recent measurements by Scholes.[27] The increase in the picosecond time scale is due to carrier trapping at the interface as we discussed in our prior work.[13]

Interestingly, we find that the "direct" transitions $X(h_1,e_1)\rightarrow XX(h_1h_1,e_1e_1)$ [line B_1 in Fig. 3(b)] and $X(h_2,e_1)\rightarrow XX(h_2h_2,e_1e_1)$ (lines B_4 and B_6) are rather strong. In contrast, the "indirect" transitions $X(h_1,e_1)\rightarrow XX(h_1h_2,e_1e_1)$ and $X(h_2,e_1)\rightarrow XX(h_1h_1,e_1e_1)$ (lines B_2, B_3, B_5, B_7, and B_8) are generally weak. Furthermore, the indirect transitions can be lower in energy than the direct transitions, i.e., B_5 is lower in energy than B_1 and B_2 is lower than B_6. This suggests the possibility of a unique contribution to the global XX Stokes shift: the $X\rightarrow XX$ absorption is weighted more heavily toward the higher-energy direct transitions, whereas the $XX\rightarrow X$ emission is weighted more heavily toward the lower-energy indirect transitions, provided that the (h_1h_2,e_1e_1) emissive states are thermally populated. For a $R=1.9$ nm CdSe nanocrystal, we find that the magnitude of such shift is ~ 4 meV [Fig. 3(b)].

While calculated global Stokes shifts δ_X and δ_{XX} are smaller than the experimental ones, all the trends of size dependence and time dependence are reproduced. One possibility for deviation is that the calculations consider only electronic effects, whereas the measured absorption and emission spectra may have contributions from phonon-progression effects. Early calculations have shown that the inclusion of LO phonon replicas increases the X global Stokes shift.[1–3] In contrast, recent experiments have suggested that the coupling to optical and acoustic phonons is very small (~ 1 meV).[26,28,29] The data in Fig. 3(c) do show small quantum beats, reflecting LO phonons. However, the phonon contribution to the data is clearly small relative to the slowly varying electronic response, consistent with a majority contribution from the electronic effects discussed here.

In summary, we report on the experimental observation of a biexciton global Stokes shift, which is significantly larger than the single-exciton global Stokes shift. We also find that the apparent biexciton binding energies measured in absorptive and emissive experiments fundamentally differ because of the different states being probed. Atomistic pseudopotential calculations show that the electronic contribution to the global XX Stokes shift is almost twice as large as the global X Stokes shift. Observation of the XX substructure and Stokes shift is important to advance our understanding of the electronic structure of multiexcitons in quantum dots and ultimately to determine how many-body interactions control optical gain and multiple exciton generation in quantum dots.

At McGill financial support from the CFI, NSERC, and FQRNT is acknowledged. R.R.C. acknowledges support from FQRNT. S.L.S. acknowledges support from McGill University. Work at NREL was funded by the U.S. DOE, SC, BES under Contract No. DE-AC36-99GO10337 to NREL.

*Authors to whom correspondence should be addressed: pat.kambhampati@mcgill.ca; alex_zunger@nrel.gov; alberto_franceschetti@nrel.gov

[1] V. I. Klimov, Annu. Rev. Phys. Chem. **58**, 635 (2007).
[2] A. L. Efros *et al.*, Phys. Rev. B **54**, 4843 (1996).
[3] D. J. Norris *et al.*, Phys. Rev. B **53**, 16347 (1996).
[4] D. J. Norris and M. G. Bawendi, Phys. Rev. B **53**, 16338 (1996).
[5] A. Franceschetti *et al.*, Phys. Rev. B **60**, 1819 (1999).
[6] G. Bester *et al.*, Phys. Rev. B **67**, 161306(R) (2003).
[7] V. I. Klimov *et al.*, Nature (London) **447**, 441 (2007).
[8] J.-Michel Caruge *et al.*, Phys. Rev. B **70**, 085316 (2004).
[9] C. Bonati *et al.*, Phys. Rev. B **71**, 205317 (2005).
[10] M. Achermann *et al.*, Phys. Rev. B **68**, 245302 (2003).
[11] U. Woggon, Springer Ser. Solid-State Sci. **146**, 107 (2004).
[12] S. L. Sewall *et al.*, Phys. Rev. B **74**, 235328 (2006).
[13] S. L. Sewall *et al.*, J. Chem. Phys. **129**, 084701 (2008).
[14] J. Shumway *et al.*, Phys. Rev. B **63**, 155316 (2001).
[15] M. Ediger *et al.*, Nat. Phys. **3**, 774 (2007).
[16] R. R. Cooney *et al.*, Phys. Rev. Lett. **102**, 127404 (2009).
[17] V. I. Klimov *et al.*, Science **290**, 314 (2000).
[18] V. D. Kulakovskii *et al.*, Phys. Rev. Lett. **82**, 1780 (1999).
[19] V. Troncale *et al.*, J. Appl. Phys. **101**, 081703 (2007).
[20] A. Malko *et al.*, Phys. Rev. B **72**, 195332 (2005).
[21] I. A. Akimov *et al.*, Phys. Rev. Lett. **96**, 067401 (2006).
[22] I. A. Akimov *et al.*, Appl. Phys. Lett. **81**, 4730 (2002).
[23] R. D. Schaller *et al.*, Nat. Phys. **1**, 189 (2005).
[24] A. Shabaev *et al.*, Nano Lett. **6**, 2856 (2006).
[25] A. Franceschetti *et al.*, Nano Lett. **6**, 2191 (2006).
[26] See EPAPS Document No. E-PRBMDO-80-R29932 for additional experimental and theoretical details. For more information on EPAPS, see http://www.aip.org/pubservs/epaps.html.
[27] V. M. Huxter *et al.*, J. Phys. Chem. B **109**, 20060 (2005).
[28] D. M. Sagar *et al.*, Phys. Rev. B **77**, 235321 (2008).
[29] G. Chilla *et al.*, Phys. Rev. Lett. **100**, 057403 (2008).